EUROPEAN ORGANIZATION FOR NUCLEAR RESEARCH

CERN–SPSC/2001–017
SPSC/P322
1 May 2001

Proposal for hadron production measurements using the NA49 detector for use in long-baseline and atmospheric neutrino flux calculations

M.G. Catanesi, E. Radicioni
Università degli Studi e Sezione INFN, Bari, Italy

T. K. Gaisser
Bartol Research Institute, University of Delaware, Newark, DE, USA

J. Bracinik, V. Cerny, M. Kreps, M. Pikna, B. Sitar
Comenius University, Bratislava, Slovakia

D. Barna, P. Csató, Z. Fodor, F. Sikler, J. Sziklai, D. Varga, G. Veres, G. Vesztergombi
KFKI Research Institute for Particle and Nuclear Physics, Budapest, Hungary

B.C. Choudhary, D.G. Michael, S. Shevchenko
California Institute of Technology, Pasadena, CA, USA

F. Dydak, H.G. Fischer, A. Grant, J. Panman, S. Wenig**, P. Zucchelli
CERN, Geneva, Switzerland

J. Bartke, E. Górnicki, A. Rybicki
Institute of Nuclear Physics, Cracow, Poland

S.V. Afanasiev, V.I. Kolesnikov, A.I. Malakhov, G.L. Melkumov
JINR, Laboratory of High Energy, Dubna, Russia

I. Boyko, G. Chelkov, D. Dedovitch, M. Gostkin, A. Jemtchougov, Z. Kroumchtein, M. Nikolenko, E. Rogalev
JINR, Dzhelepov Laboratory of Nuclear Problems, Dubna, Russia

L. Betev, P. Bunčić, R. Renfordt, R. Stock
Fachbereich Physik der Universität, Frankfurt, Germany

A. Lebedev, M.D. Messier
Harvard University, Cambridge, MA, USA

R. Nichol, J. Thomas, D. Tovee
University College London, London, UK

C. Höhne, F. Pühlhofer
Fachbereich Physik der Universität, Marburg, Germany

M. Bonesini, M. Paganoni, A. Tonazzo
Sezione INFN, Milano and Università Milano-Bicocca, Italy

V. Palladino
Università "Federico II" e Sezione INFN, Napoli, Italy

G. Barr*, A. De Santo, B. Raeven, A. Weber
University of Oxford, Oxford, UK

A. Guglielmi
Università degli Studi e Sezione INFN, Padova, Italy

T. Patzak
College de France, Paris, France

V. Ammosov, A. Semak
Institute for High Energy Physics, Protvino, Russia

U. Dore
Università "La Sapienza" e Sezione INFN Roma I, Rome, Italy

R. Edgecock
Rutherford Appleton Laboratory, Chilton, Didcot, Oxon, UK

C.N. Booth, P. Hodgson
University of Sheffield, Sheffield, UK

N. Darmenov, A. Dimitrov, D. Kolev, L. Litov, M. Makariev, M. Mateev, S. Stoinev
M. Tchijov, R. Tzenov
St. Kliment Ohridski University, Sofia, Bulgaria

V. Genchev, I. Damgov, P. Vankov
Institute for Nuclear Research and Nuclear Energy, Bulgarian Academy of Sciences, Sofia, Bulgaria

S. Affakumov, L. Wai, S.G. Wojcicki
Stanford University, Stanford, CA, USA

E. Falk, P.G. Harris
University of Sussex, Falmer, Brighton, UK

S. Kopp, K. Lang
University of Texas at Austin, Austin, TX, USA

H. Białkowska, B. Boimska
Institute for Nuclear Studies, Warsaw, Poland

K. Kadija, T. Susa
Rudjer Boskovic Institute, Zagreb, Croatia

* Spokesperson
** Contact person

Contents

1 Introduction

The experiments on solar and atmospheric neutrinos provide strong evidence for physics beyond the Standard Model. More specifically, the deficit of solar neutrinos observed on Earth, deduced from comparison with the solar model predictions, suggests oscillations of ν_e into some other flavor. The atmospheric neutrinos provide even stronger evidence for the existence of neutrino oscillations, since the observed deficit of muon neutrinos shows dependence on the zenith angle of the observed neutrinos, and hence on their path length from the production point to the observation point.

Understanding the mechanisms responsible for these observed phenomena in a quantitative way is of paramount importance. Several accelerator neutrino experiments, K2K in Japan, OPERA and ICARUS in Europe, and MINOS in the United States have been initiated with the goal of understanding the atmospheric anomaly quantitatively. New ideas have been put forth regarding possible next generation atmospheric neutrino experiments.

Both the neutrinos produced in the atmosphere and the neutrinos in accelerator beams originate as decay products of mesons (mainly pions and kaons) or of muons, which themselves are primarily pion or kaon decay products. Thus understanding of the atmospheric neutrino fluxes as well as of the detailed composition of the accelerator neutrino beams relies heavily on understanding the nature of the hadronic cascade, i.e. the production spectra of the secondaries resulting from the collision of a higher energy particle. The existing data on this topic are presently rather limited and this lack of information is currently the largest source of uncertainty in the quantitative interpretation of the atmospheric neutrino data. Furthermore, the precision of the forthcoming MINOS experiment may well be limited by the accuracy of the predictions of the neutrino fluxes at the far detector (in the absence of oscillations) based on observations in the near detector. This extrapolation of the neutrino energy spectrum is a strong function of the details of the production spectra of the secondary pions and kaons.

We propose to perform a dedicated experiment to measure the secondary hadron production spectra in a kinematical region of interest both to atmospheric neutrino experiments and to MINOS (and possibly OPERA and ICARUS). This experiment would extend the kinematical region probed to energies above those that are studied by the HARP experiment. Most of the data would be taken with thin targets so that direct information would be obtained on the secondaries produced in the collision of the primary projectile.

Independent of the usefulness of these data to MINOS and atmospheric neutrino experiments, the data will have significant physics value in its own right. Most of the high energy physics experiments today rely very heavily in their design and interpretation on simulation programs, like GEANT. The quality of many GEANT calculations, in turn, relies very heavily on good knowledge of the hadronic production spectra. Thus the measurements we are proposing to make would also be of benefit to the high energy physics community at large.

Currently there exists a detector at CERN which is capable of performing the required measurements, namely the NA49 apparatus, shown in Figure 1. Furthermore, this detector is located in a beam which is capable of providing particles of interest to our Collaboration. We plan to take advantage of these very fortuitous circumstances and use

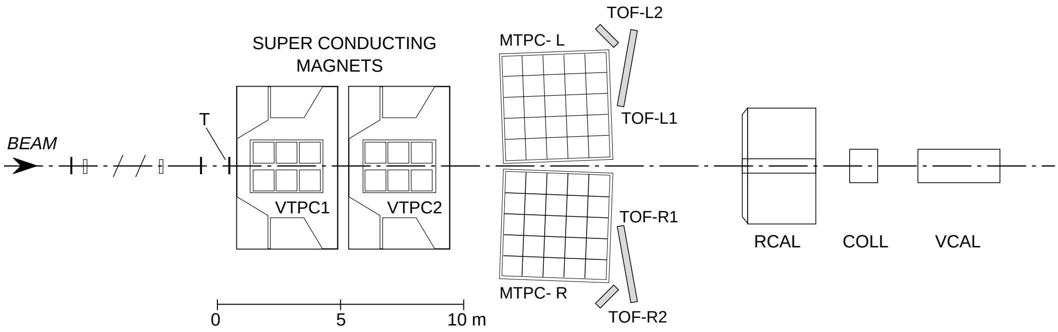

Figure 1: Schematic of the NA49 detector

this setup for our measurements.

Some of the important features of the NA49 experimental apparatus which make it almost ideal for our purpose are: large solid angle acceptance; time projection chambers (TPC) allowing precise particle tracking and particle identification up to 80 GeV via dE/dx sampling; time of flight counters with 60 ps resolution, covering the geometrical region intercepted by particles with momenta below 10 GeV/c; data acquisition system permitting adequate data rate; spatial definition of the incoming particles. The fact that the apparatus has been in use for a number of years is very important. It is fully debugged and the required associated software exists and is also fully checked out. The apparatus can be used for our experiment essentially as is, with very minor hardware modifications (target location, strength of magnetic field). Thus the use of this apparatus offers one a cost effective way of performing highly significant physics measurements.

This proposal is being submitted by a consortium of institutes, many of whom are a subset of NA49, HARP, or MINOS. All of these institutes will participate in data taking and subsequent data analysis.

2 The NA49 experiment

The NA49 experiment[1] is situated in the SPS North Area at CERN on the H2 fixed target beam line which offers secondary beams of identified protons, pions and kaons with momenta between 40 to 350 GeV/c. The experiment was designed for coping with the ∼1500 charged particles produced in central Pb+Pb collisions. To date, the NA49 experiment has also collected an appreciable amount of $p+p$ and centrality trigger-selected $p+A$ (mainly heavy nuclei) data. The large solid angle acceptance and excellent tracking and particle identification performance (even at high track densities) makes the NA49 detector an ideal tool to study collisions of proton/pion beams with light nuclei, as proposed in this note.

The layout of the main detectors (Figure 1) comprises two vertex TPCs (VTPC-1,2) followed by two main TPCs (MTPC-L,R). The two vertex TPCs are each inside a 1.5 Tesla super-conducting magnet which produces a p_T kick in the horizontal plane. This field bends most of the low momenta particles into the active TPC volume. The electrons produced along the particle trajectories drift vertically upwards to the readout chambers

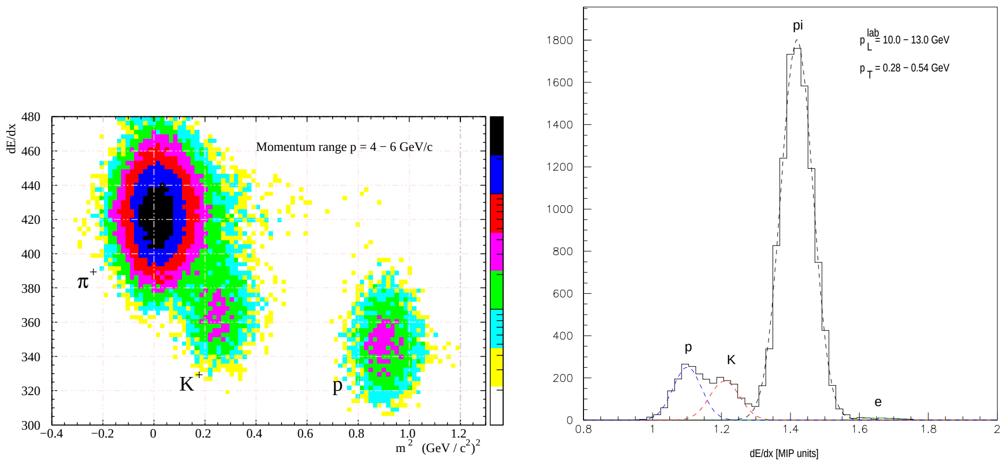

Figure 2: Left: Reconstructed dE/dx vs. m^2 for tracks in the NA49 detector accepted by the TOF system. Right: Sample dE/dx distribution with fitted positron, pion, kaon, and proton yields.

on the top of the detectors. The high granularity pad readout is shaped to follow the mean trajectory of the particles from the target. This is to aid in pattern recognition and to maximize the response for dE/dx measurements. Where the dE/dx response curves of the different particles overlap ($p \sim 4$ GeV/c), the particle ID is augmented with time-of-flight scintillation counters. Figure 2 shows the particle identification capabilities of the detector. Downstream of the main apparatus, leading particles can be identified to be either protons or neutrons using the ring calorimeter (RCAL) information in connection with the signals of two tracking chambers.

The target is positioned in front of the first TPC. A minimum bias trigger is formed in anti-coincidence with a small scintillation counter located on the beam trajectory 4 m downstream of the target. This trigger will be used for all the measurements described in this proposal.

The data acquisition is optimized for high multiplicities and consequently, is somewhat rate limited for low occupancy events. Recent experience with proton beams shows that under good running conditions data collection rates of 1×10^6 events per week can be achieved.

3 NuMI/MINOS

3.1 The MINOS experiment

The MINOS (Main Injector Neutrino Oscillation Search)[2] experiment has been designed to make precise measurements of the neutrino oscillation signals observed in underground detectors. For a two-neutrino oscillation hypothesis, the probability for a neutrino produced in an electro-weak eigenstate ν_μ to be observed in the same eigenstate after traveling a distance L through a vacuum is:

$$P_{\nu_\mu \to \nu_\mu} = 1 - \sin^2 2\theta \sin^2 \Big(\frac{1.27\Delta m^2[\mathrm{eV}^2]L[\mathrm{km}]}{E_\nu[\mathrm{GeV}]}\Big), \qquad (1)$$

where E_ν is the neutrino energy, θ is the mixing angle between the flavour eigenstates and the mass eigenstates, and Δm^2 is the mass-squared difference of the neutrino mass eigenstates. For a fixed distance between the neutrino source and the detector, neutrino oscillations will produce an energy-dependent suppression of the neutrino event rate which depends on the oscillation parameters $\sin^2 2\theta$ and Δm^2.

The NuMI (Neutrinos at the Main Injector)[3] neutrino beam will be produced by directing 120 GeV/c protons from the Fermilab Main Injector to a 94 cm long graphite target. The pions and kaons generated in these interactions will be focused using two parabolic magnetic horns into a 670 m long decay region. The neutrino beam will be directed at two detectors, one at the Fermilab site (1 km from the target) and one located 735 km from the target in northern Minnesota. The near detector will provide a high statistics measurement of the neutrino energy spectra which can be extrapolated to the far detector site using a model of the NuMI neutrino beam. The detailed comparison of the extrapolated near detector spectrum to the measured far detector spectrum will be used to fully characterize the modes and parameters of any oscillation signal which might be observed.

3.2 Uncertainties due to hadron production

One of the largest uncertainties in the extrapolation of the near detector neutrino spectra to the far detector site is due to modeling hadron production on the NuMI target. The regions of hadron phase space which contribute to the MINOS neutrino flux are shown in Figure 3. The existing relevant world data have been overlaid on the figure. The hadron production data is relatively sparse, and must be extrapolated from different target nuclei and beam momenta to be applied to the NuMI case. For these reasons, predictions of the hadron yields from the NuMI target are 20-30% uncertain. Figure 4 shows the expected MINOS neutrino event rates at the near detectors for four different hadron production models of the NuMI target. Figure 5 shows the predicted ratio of the far neutrino flux to the near neutrino flux for the same four models. The predictions differ by 10-25% in the absolute prediction and as much as 10% in the far/near ratio. A reduction in the uncertainty in the far/near ratio due to hadron production to approximately 2% would put this uncertainty on par with uncertainties in the near-far comparison due to statistics and detector systematic uncertainties.

3.3 Requirements for hadron production data

3.3.1 Acceptance

Overlaid on the $p - p_\mathrm{T}$ plot (Figure 3) are contours corresponding to particle tracks that produce on average 8 (minimum needed for track fitting), 30 (the minimum needed to form a reliable truncated mean $\mathrm{d}E/\mathrm{d}x$ and momentum measurement), and 100 TPC hits

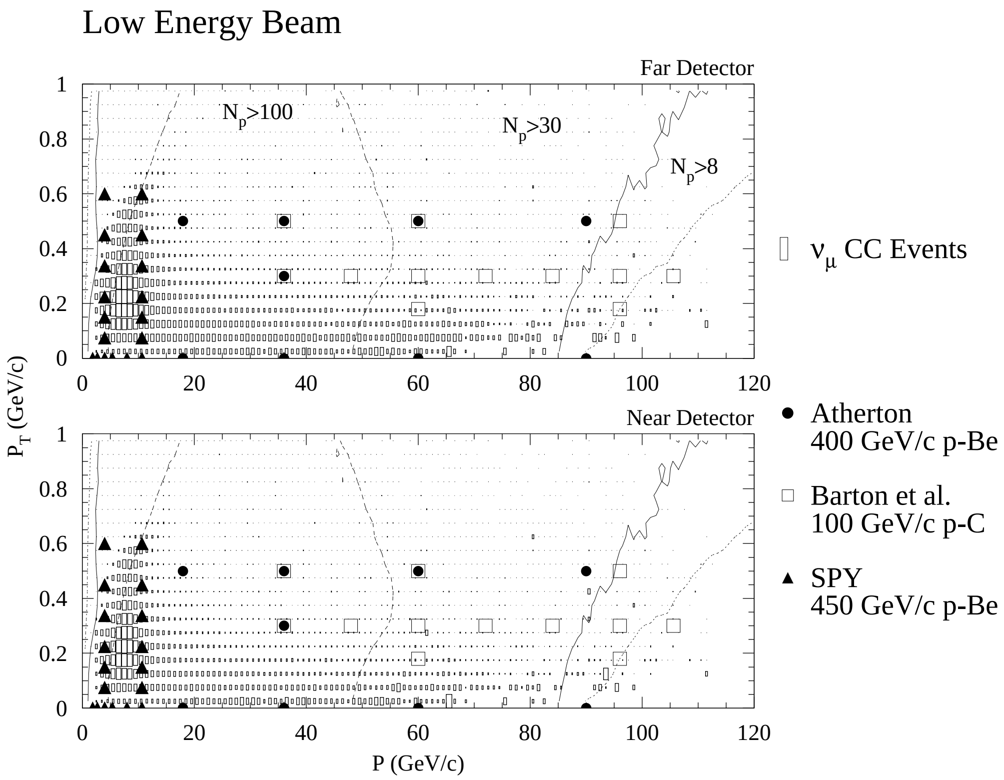

Figure 3: The distribution in p and $p_{\rm T}$ for secondary pions produced on the NuMI target. Secondaries have been weighted by their contribution to the neutrino event rate at the far (top) and near (bottom) detectors. Overlaid are the locations of existing hadron production measurements [4, 5, 6], and the contours delineating the kinematic regions in which particles traversing the NA49 apparatus have on the average at least 8, 30, or 100 TPC track points.

in the NA49 detector. The standard target and field configuration of the NA49 detector has a good acceptance for the full range of particles of interest to MINOS.

3.3.2 Particle ID

The MINOS neutrino spectra result from a combination of pions and kaons. As shown in Figure 6, the kaon contribution to the muon neutrino flux is a few percent below 5 GeV but grows to roughly 30% at 30 GeV. Using the NA49 detector, the pion, kaon, and proton yields from proton-nucleus interactions are extracted from truncated energy loss distributions in selected momentum bins, (see, for example, Figure 7). The $\mathrm{d}E/\mathrm{d}x$ fitting procedure takes full account of detector response and resolution. The systematic uncertainty introduced through this procedure depends on the overall counting statistics, and on the relative abundances of pions, kaons, and protons. It has been shown in previous NA49 measurements of kaon yields that this systematic uncertainty can be kept to a level of less than two times the statistical uncertainty of the kaon yield. Preliminary fits to

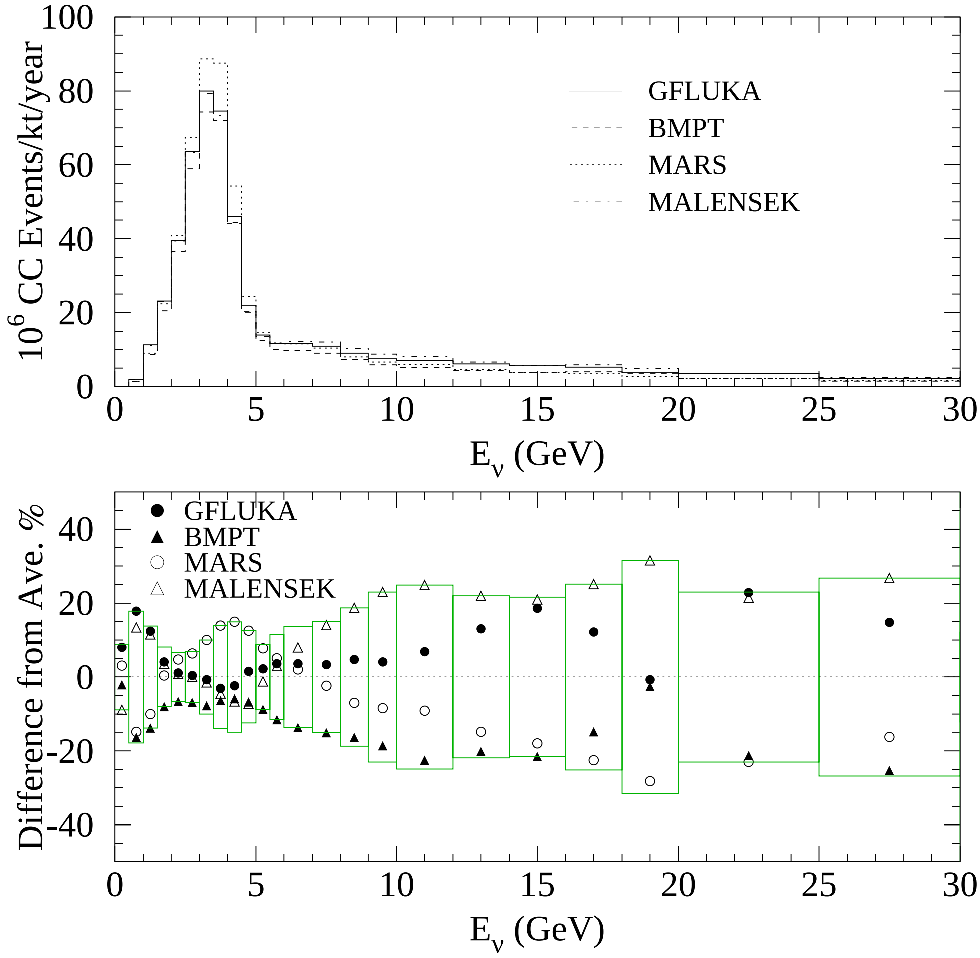

Figure 4: Predictions of the absolute neutrino rates at the MINOS near detector using four hadron production models [7, 8, 9, 10].

a small (∼40,000 events) sample of existing NA49 proton-Aluminum data are consistent with this estimate. For example, the fit to the data shown in Figure 7 yielded 92±11% pion and 39±25% kaon tracks. Statistical uncertainty alone would give a 16% error in kaon rate suggesting that the uncertainty due to other parameters of the dE/dx fit contribute $\sqrt{25^2 - 16^2} = 19\%$. Taking the π/K uncertainty for the larger data samples proposed conservatively at 15%, the uncertainty in the π/K ratio would contribute at most (30% × 15%) $\simeq$ 5% to the uncertainty in the absolute MINOS neutrino fluxes at high energy. This level of precision should be adequate to limit the uncertainty due to π/K separation in the near-far extrapolation to 2% over the full neutrino energy range.

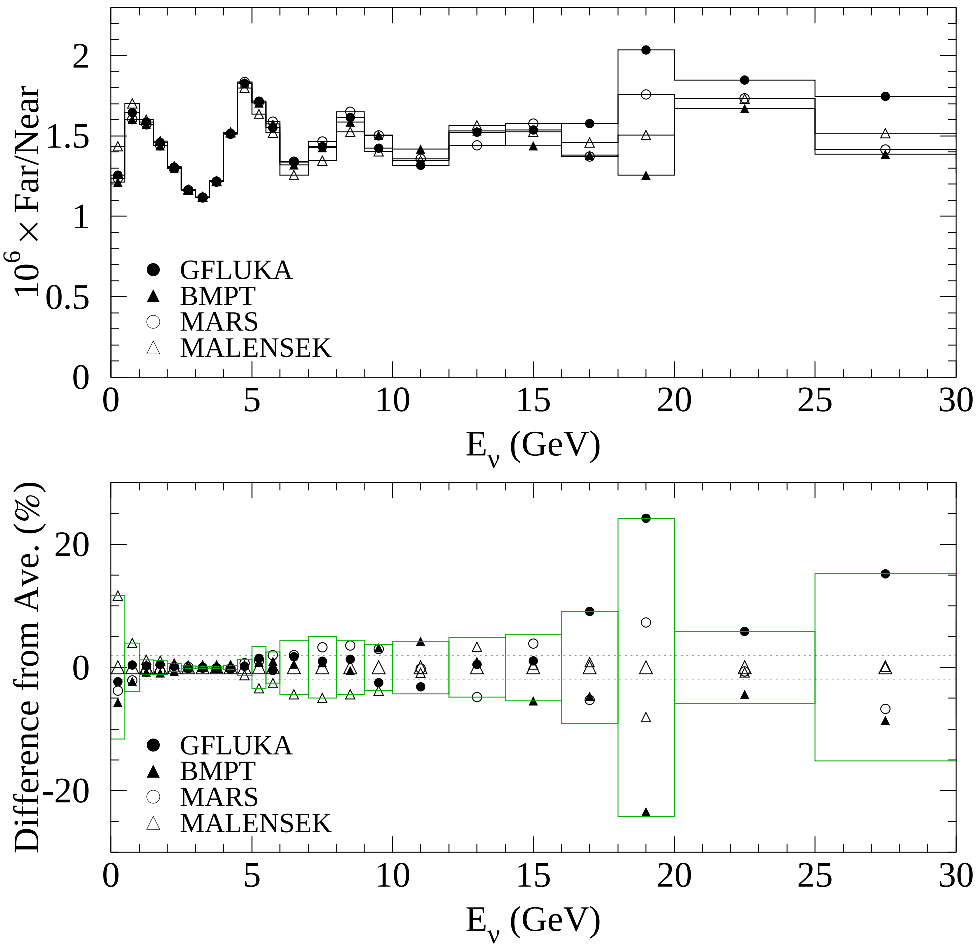

Figure 5: The predictions for the ratio of the far neutrino flux to the near neutrino flux using the same four models as Figure 4.

3.3.3 Modeling the NuMI target

The target used to produce the NuMI beam is shown in Figure 8. The target is composed of 47 segments of graphite of 2 cm in length for a total length of 94 cm (1.9 interaction lengths). While the final goal is to understand the production of hadrons on this target, it is impractical to place the exact NuMI target in front of the NA49 detector as the proton beam spot size and divergence are significantly different from those of the proton beam at the Main Injector. Instead, the proposed approach is to make the fundamental measurements of proton-Carbon interactions (using thin targets) which can be used to build an accurate parametric model of hadron production on the NuMI target.

As the NuMI target is 1.9 interaction lengths long, the prediction of the total particle yields must account not only for the interactions of the primary protons, but also the re-interactions of hadrons inside the target. The contribution from secondary and tertiary

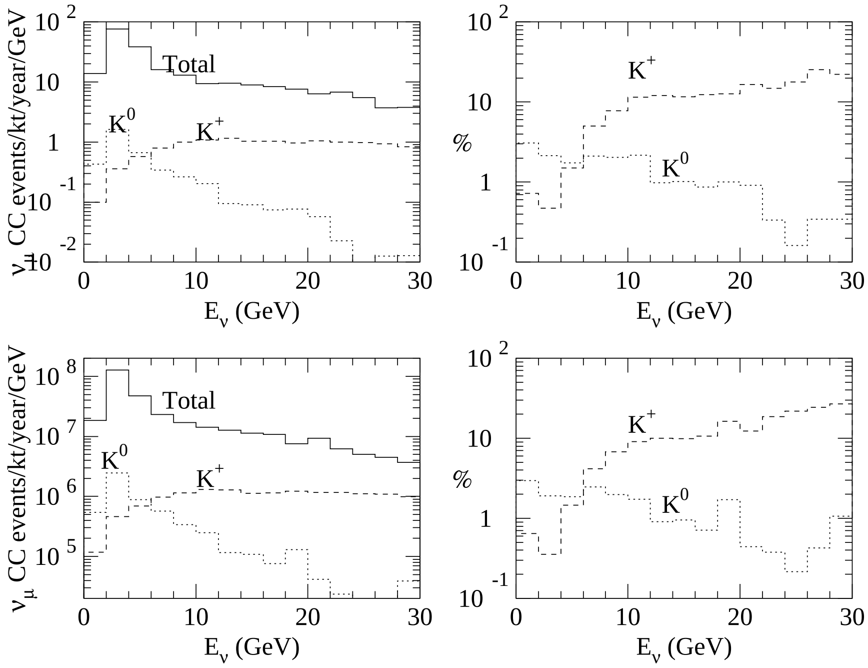

Figure 6: Fraction of ν_μ produced from kaons in the NuMI beam. Results for both the far detector (top) and near detector (bottom) locations are shown.

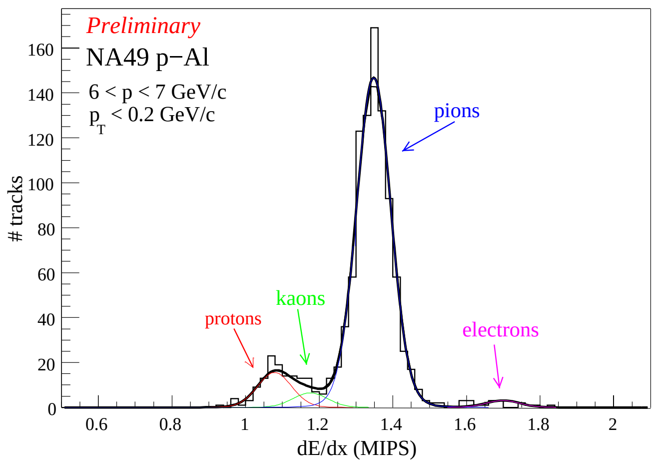

Figure 7: Fits to dE/dx distributions for existing p-Al data.

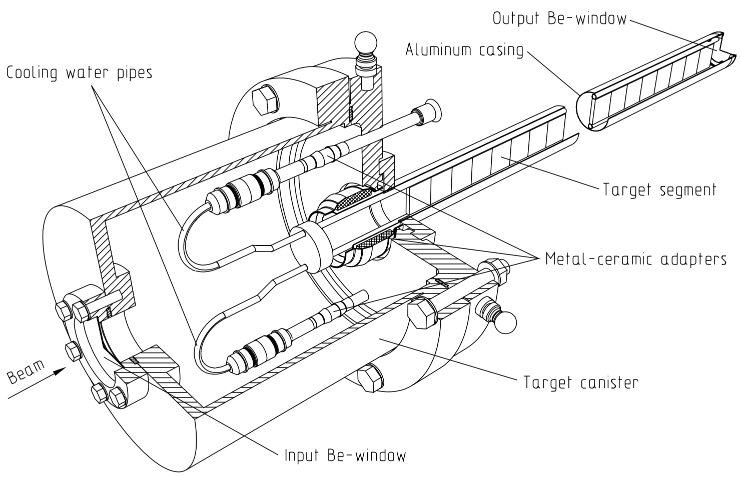

Figure 8: The NuMI target.

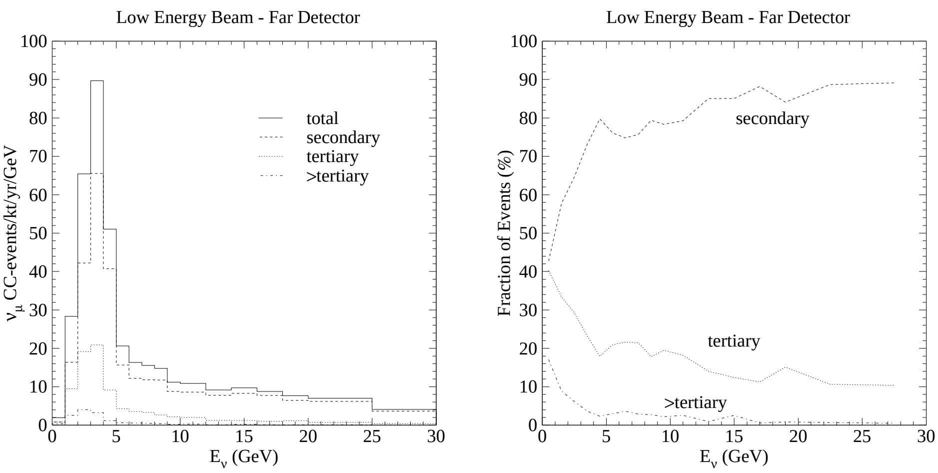

Figure 9: Left: The contributions to the muon neutrino event rate measured at the far detector resulting from secondary, tertiary, and higher generation particles produced in p-C interactions in the 94 cm NuMI target. Right: The fractional contribution of the different generations to the neutrino spectrum as a function of energy.

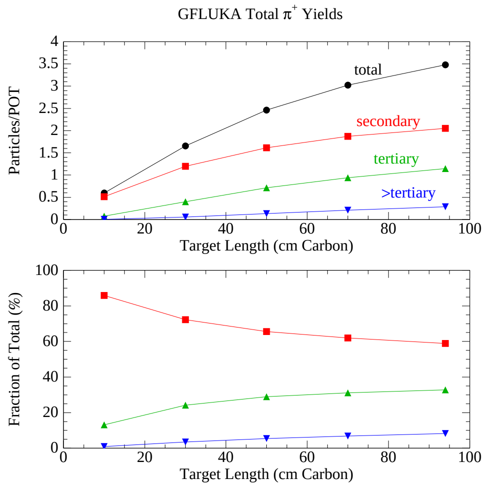

Figure 10: The estimated yield of secondary and tertiary particles as a function of target length

hadrons to the MINOS neutrino fluxes is shown in Figure 9. At low energies, roughly 40% of the total neutrino flux results from tertiary or higher generation particles. At higher energies this fraction is still quite significant accounting for roughly 20% of the neutrino flux. Tertiary particles are produced by interactions of secondary protons (40%), pions (30%), neutrons (20%), and a small fraction of kaons. Thus, the complete understanding of the NuMI target will require input on the hadronic shower development in thick targets. For this reason, we propose to take proton-Carbon and pion-Carbon data at lower energies to cover the energy range above the HARP [11] experiment at CERN. We also plan to make measurements using longer (∼50% – 100%) interaction length targets in addition to the 2% targets. As shown in Figure 10, the hadron spectra produced on targets in this length range should be ∼20–30% from tertiaries. These data points will enable us to tune the the yields of tertiary and higher generation particles in the target model. The running conditions are summarized in Table 1 in Section 6.1. The exact choice of target thicknesses will be optimized over the coming year.

4 Atmospheric neutrinos

4.1 Introduction to atmospheric neutrinos

The observation of oscillation of atmospheric neutrinos in underground detectors [12] derives from the measurement of a deficit of muon type neutrinos produced by the interaction of cosmic rays in the upper atmosphere on the opposite side of the earth to the detector (i.e. the ones coming upward having traversed about 10^4 km since production). This deficit is established by comparing with either the rate of muon-neutrinos produced in the atmosphere locally (i.e. the ones going downward) or with the rate of electron-neutrinos.

The lack of an accurate prediction of the atmospheric neutrino fluxes does not affect the conclusion that oscillations exist. However, improving the flux predictions is imperative for a detailed understanding of the measured distributions, for example, to gain a refined knowledge of the path-length distribution, and to verify that the absolute rate of electron-neutrinos can be understood.

Neutrinos of energies around 1 GeV are responsible for the signals seen in contained events underground (the muon (electron) momentum threshold in the Super–Kamiokande analysis is 200 (100) MeV/c). Analyses of upward through-going muons such as those at the MACRO and AMANDA experiments are sensitive to neutrinos with much higher energies, in the range 10 GeV to 1 TeV.

Atmospheric flux calculations proceed by inserting the measured cosmic ray fluxes into a Monte Carlo calculation which generates hadronic cascades and collates the number of neutrinos produced from the resulting mesons and subsequent decay muons. A detailed model of the geomagnetic field is used. These calculations also predict the atmospheric muon fluxes, and in particular, the high altitude muon fluxes provide an important cross check for the calculations. Calculations include work performed by the Bartol group [13], Honda *et al.*[14] and Battistoni *et al.*[15]. Comparisons between these and other flux calculations are given for example by Lipari [16] and Battistoni [17]. The fluxes are currently known to a level of about 30% and the ratio of fluxes needed in the comparisons in Super–Kamiokande described above to about 7%.

The uncertainty in predicting underground interaction rates of neutrinos comes from three sources:

- The flux of primary cosmic ray protons and heavier nuclei has in the past been known to only about 25%. This was primarily due to a 50% inconsistency between measurements in the most important primary energy range around 20 GeV. Recent high precision measurements [18] from IMAX, CAPRICE, BESS, MASS and AMS have resolved this problem and also significantly improved the precision. Primary cosmic ray fluxes are now known to better than 10%.

- The lack of adequate data to construct a reliable hadron interaction model which is realistic over the whole range of kinematic parameters. HARP will make new measurements of the particle yields at incident particle energies of up to 15 GeV. This proposal addresses the extension of these measurements to higher energies.

- Uncertainties in the neutrino cross sections. At low energies, quasi-elastic interactions dominate and nuclear reinteraction generates uncertainties of about 15%.

Nuclei comprise approximately 25% of the cosmic ray flux. Thus hadroproduction from neutrons (currently obtained from protons using isospin symmetry) and nuclear effects must be modelled carefully. HARP proposes [19] to measure hadroproduction with helium ions as projectiles to accurately quantify these effects.

4.2 Measurements for atmospheric neutrino fluxes

The current experimental situation for hadroproduction for atmospheric neutrino interactions is reviewed by Engel *et al.* [20]. To summarize, there are many measurements of various small subsets of the required phase space (as illustrated in Figure 3) which require

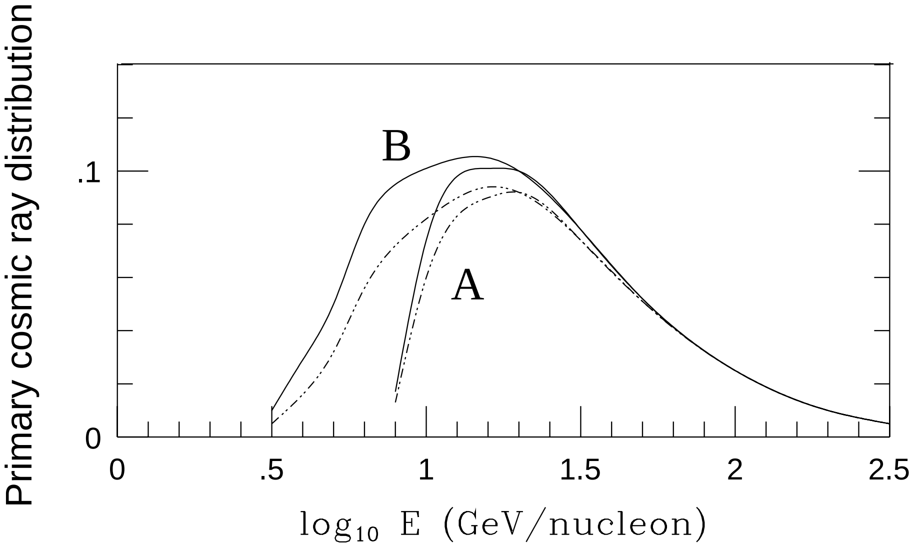

Figure 11: Energy distribution of the primary cosmic-ray nucleons giving rise to sub-GeV neutrino interactions in Super–Kamiokande. Curve A is for cosmic rays in the local atmosphere at Kamioka (neutrinos from above the horizon) which are affected by the strong horizontal geomagnetic field in that region of the world. Curve B is for cosmic rays giving rise to neutrinos from below the horizon (average geomagnetic effect over the earth). Each pair of curves shows the variation of the signal between solar activity minimum (the upper curve) and maximum (the lower curve).

major model-dependent extrapolation to get the overall information required - this leads to the 30% uncertainty in the overall atmospheric fluxes. Experiments are typically either a single arm spectrometer (which measure only very few angles, usually close to 0°), or an emulsion experiment which measures all directions, but not the momenta of the particles.

The most important information required for the calculation of the fluxes is the measurement of hadroproduction over the entire phase space as a function of the magnitude of the final state meson momentum at a number of suitable primary energies. In particular, we must determine how many particles are produced with energy of 10% of the primary energy, a quantity which is essentially unconstrained by current measurements.

This information is needed from proton collisions with nuclei whose size is close to that of air ($A \simeq 14$). The strategy proposed here is to take the majority of the data with carbon targets ($A = 12$) and a few points with an aluminium target ($A = 27$) and interpolate to provide the measurements for air. In this way, target handling is simple and most of the measurements overlap with the MINOS measurements. However, we retain the option of using cryogenic N_2 targets with the HARP cryogenic target equipment. This choice will be made based on the experience with cryogenic targets in HARP running in 2001.

The energies of the protons responsible for the sub-GeV sample in Super–Kamiokande are shown in Figure 11 from [20], indicating that about 50% of the signal is from protons

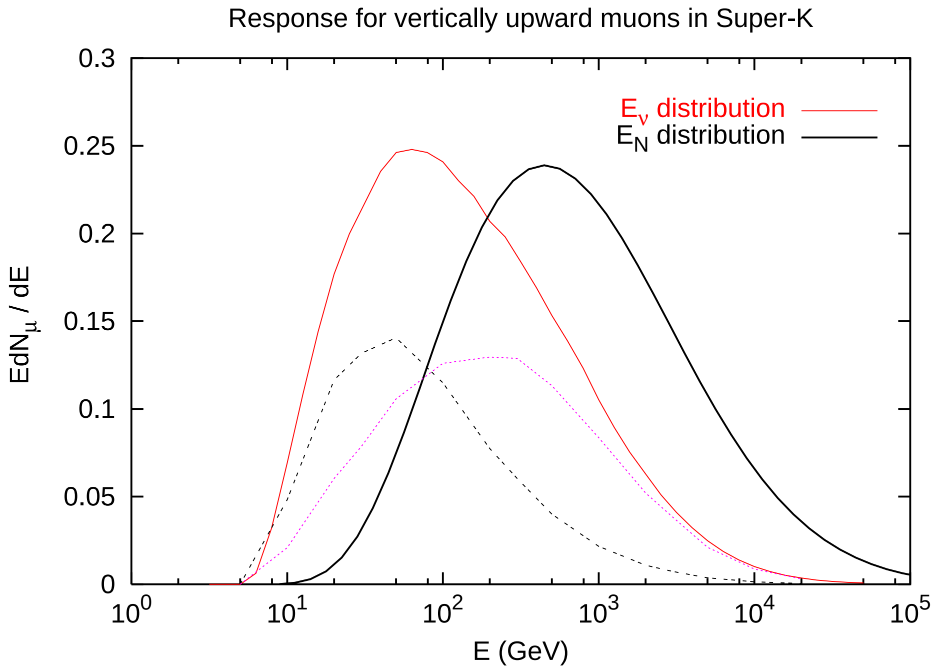

Figure 12: Distribution of neutrino energy (light solid) and primary nucleon energy (heavy solid) that produces the signal of through-going upward muons at Super–Kamiokande. Each curve is normalised to unity. The contributions to the neutrino energy distribution from pions (double dash) and of kaons (dotted) are shown.

with energy above 15 GeV (the maximum HARP energy), continuing to above 100 GeV. Figure 12 from [18] indicates the primary energies and neutrino energies responsible for the vertical through-going muon signal in underground detectors. Protons in the range 100 GeV to 10 TeV are responsible for these neutrinos which have energies between 10 GeV and 1 TeV. We therefore need to measure from the lowest practical beam momentum, which is 40 GeV/c in the H2 beam line, to the highest momentum available (around 350 GeV/c, since for radiation reasons, the beam line is limited to secondary beams). A large sample of data will be collected at one momentum which is most conveniently chosen to be the data suitable for the MINOS studies at 120 GeV/c.

Figure 13 shows the distribution of all pions produced in the forward direction in the laboratory frame in hadron interactions at 120 GeV/c. Approximately 10% of particles emerge backwards and are not in the acceptance of NA49. Pions below about 0.5 GeV/c are uninteresting as they produce neutrinos which are below detection threshold. The particles of interest are similar to the ones for the MINOS measurements. However, they extend to lower momenta where large numbers of pions are produced which are important for atmospheric neutrinos but are not accepted into the NuMI decay channel.

Figure 14 shows the regions of the ($p_{\rm L}$,$p_{\rm T}$) plane where the acceptance is good based on the total number of samplings in the TPCs along the track. This has been obtained by applying a 'ϕ-wedge' cut in the azimuthal angle of the emerging secondary particles to select the ones which bend into the TPCs. There is a wide region of the phase space where

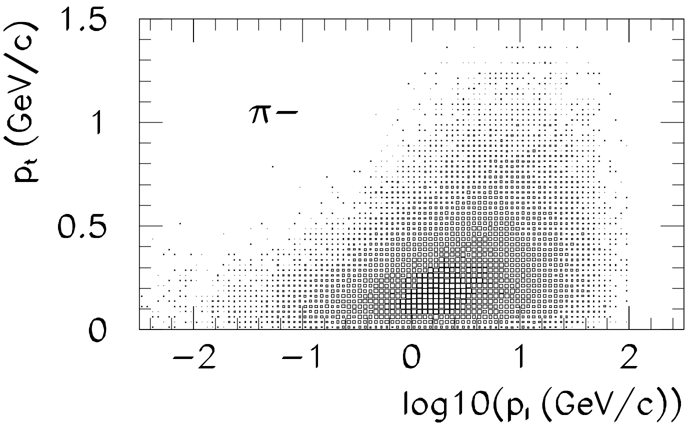

Figure 13: The momentum distribution of pions produced from protons at 120 GeV/c.

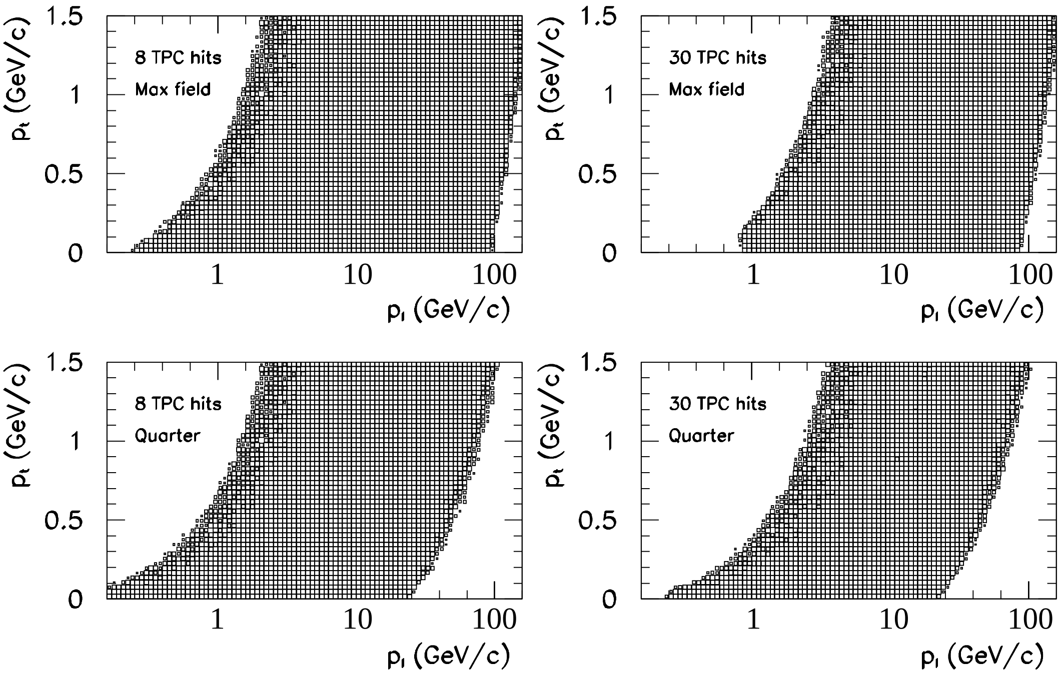

Figure 14: The acceptance of NA49. The left (right) hand plots show the acceptance which gives a sufficient number of TPC samplings for track (dE/dx) reconstruction. The top row of plots are for the nominal configuration and the lower plots show how the acceptance changes as the magnetic field is reduced.

the acceptance is 100% which is ideal for performing measurements with low systematic errors. In addition, there are large regions of p_L for which essentially the complete p_T distribution is measured (from the data in Figure 13, 95% (60%) of the particles have a p_T less than 0.7 GeV/c (0.3 GeV/c)). The top-left plot of Figure 14 shows the acceptance of tracks required to have a minimum of 8 TPC samplings which is sufficient to reliably reconstruct the track. This is possible for 60% of the p_T distribution for p_L between 0.6 GeV/c and 90 GeV/c.

Particle identification is important, particularly to remove protons from the analysis. The top-right hand plot of Figure 14 shows the acceptance of tracks required to have at least 30 TPC samplings which is the minimum to make a $\mathrm{d}E/\mathrm{d}x$ measurement on the track. This is possible for 60% of the p_T distribution for p_L between 1.3 GeV/c and 85 GeV/c.

In order to improve acceptances at low values of p_L, we can lower the magnetic field. The bottom plots on Figure 14 show the change in acceptance when the field is lowered to a quarter of its nominal value. This allows acceptance of 60% of the p_T distribution down to $p_L = 0.5$ GeV/c for tracking (the lower limit of interesting pions from the point of view of neutrino detectors) and $\mathrm{d}E/\mathrm{d}x$ measurement to 0.8 GeV/c. Improvements in the fraction of the p_T distribution are possible by moving the target forward and by accepting particles outside the ϕ-wedge.

Due to differences in kaon and pion decay kinematics and to the steeply falling primary cosmic ray spectrum, kaons become increasingly important for neutrino fluxes for E_ν above 100 GeV, i.e. for through-going muon fluxes [18]. This is shown in Figure 12 where the neutrino energy spectrum is subdivided into neutrinos originating from kaons and pions separately. A determination of the fraction of kaons produced is thus important, particularly at higher energies.

4.3 Measurements required

The programme of measurements is made as short as possible, due to the limited time in the H2 beam line and the NA49 DAQ system. We propose to make extensive measurements on carbon at only one point, 120 GeV/c (overlapping with the data to be collected for the MINOS studies) to obtain good statistics over the entire particle production phase space and shorter measurements at 40, 70, 200 and 350 GeV/c to obtain good statistics in the regions where copious particle production occurs. The low energy points are measured twice (a) with the nominal configuration of target position and magnetic field and (b) a short run with a quarter of the nominal field and the target moved close to the TPC. This provides maximum coverage of the phase space, and also makes possible a systematic check of the measurements at intermediate momenta in two separate physical regions of the detector. All measurements will be with the thin target. Short runs with an aluminium target are also foreseen at 40 GeV/c and 120 GeV/c. The running conditions are summarized in Table 1 in Section 6.1.

5 Hadronic event generators

Hadronic event generators have become an indispensable tool in particle physics simulations. Their applications are as diverse as Monte Carlo calculation of acceptances, estimation of backgrounds, energy resolution of calorimeters, fluxes of neutrino beams, shielding calculations, and radiation levels in materials exposed to intense particle fluxes. Monte Carlo techniques facilitate the simulation of hadronic final states, and have been developed for many years.

Three types of modeling are used in current hadronic event generators: data-driven, parametrization-driven, and theory-driven modeling. Data-driven modeling is known to provide the best approach to low energy neutron transport, isotope production and nuclear radiative decays, needed for studies of intense irradiation of materials. Parametrisation-driven modeling permits easy tuning of hadronic shower development and is widely used for calorimeter simulation. Theory-driven modeling promises a reasonable extrapolation of results to presently unaccessible energies. However, no matter which of the three approaches is used, the role of accurate experimental data is fundamental in preparing accurate hadronic event generators.

In Europe, the codes most often used are FLUKA [21], GEANT3 [7] and GEANT4 [22]. Their counterpart in the USA is MARS [9]. The codes are continuously developed driven by the desire and need to describe experimental data as accurately as possible.

The 1992 version of FLUKA is incorporated as G–FLUKA in the general-purpose GEANT Monte Carlo programs. Other GEANT options are G–GHEISHA [23] and G–CALOR [24]. It is common practice that different generators are used for different applications, and no commonly accepted answer exists yet as to which the 'best' hadronic generator is.

In order to assess differences between hadronic generators, A. Ferrari and P.R. Sala studied the responses of G–FLUKA, G–GHEISHA, G–CALOR and FLUKA in various interactions [25]. They studied conservation of charge, baryon number, energy, and momentum; azimuthal distributions, multiplicities, and Feynman–x and p_{T}^2 distributions. Significant differences were found, predominantly at projectile particle energies of a few GeV. At higher energy, inclusive particle distributions are experimentally much better known, yet there remain significant differences as shown in Figure 15 taken from [25]. The large differences between different hadronic generators are clearly visible.

G. Collazuol *et al.* [26] have compared hadronic production between experimental data from SPY [6] and from Atherton *et al.* [4] with the predictions of FLUKA, G–FLUKA and G–GEISHA. For example, Figure 16 shows the longitudinal momentum distributions of π^+ and K^+ produced in 450 GeV/c proton–beryllium collisions. The authors conclude that FLUKA reproduces the available data correctly (and hence generates a trustworthy neutrino flux for the beam from CERN to Gran Sasso), while G–FLUKA overestimates the hadronic production (and hence predicts too high a flux of muon-neutrinos by 15–20%). G–GEISHA predictions are considered unacceptable.

Both for the atmospheric neutrino flux and for the prediction of the neutrino flux from the NuMI target, a correct description of the hadronic production is of importance. The good agreement of FLUKA with data is due to *a posteriori* 'tuning' of parameters which underlines the relevance of data. The precise measurements proposed in this document

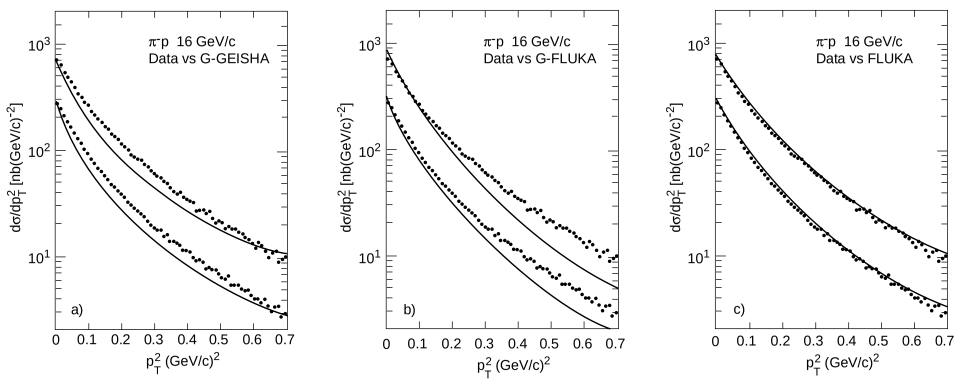

Figure 15: p_{T}^2 distributions from 16 GeV/c π^- on protons. Full circles refer to experimental data, lines refer to hadronic event generators; left: G–GHEISHA; middle: G–FLUKA; right: FLUKA.

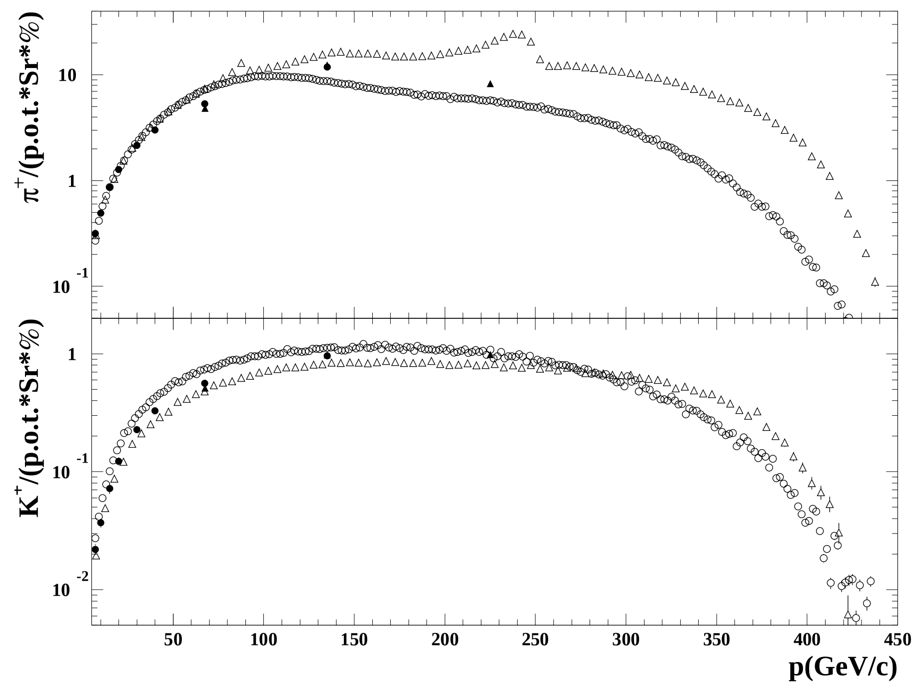

Figure 16: Longitudinal momentum distributions of π^+ and K^+ produced in 450 GeV/c proton–beryllium collisions, for forward angles less than 0.2 mrad; open circles: FLUKA; open triangles: G–FLUKA; full circles and triangles: experimental data.

Beam type	Momentum (GeV/c)	Target material	Thickness (int. len.)	Magnetic field	# triggers $\times 10^5$
p	40	C	2%	Nominal	10
π	40	C	2%	Nominal	10
p	40	C	2%	Low	5
p	40	Al	2%	Nominal	5
p	70	C	2%	Nominal	5
p	70	C	2%	Low	5
p	120	C	2%	Nominal	25
p	120	C	50%	Nominal	10
p	120	C	100%	Nominal	10
p	120	C	2%	Low	5
p	120	Al	2%	Nominal	5
p	200	C	2%	Nominal	5
p	350	C	2%	Nominal	5

Table 1: List of proposed data points to be taken with the NA49 detector.

will make an important contribution towards these goals. More generally, the same measurements will considerably enhance, in conjunction with the data that will come from the HARP experiment at the CERN PS, the reliability of future public versions of hadronic generators, for whatever good use they may serve.

6 Schedule and resources

6.1 Measurement programme

Table 1 lists the proposed series of measurements. It is assumed that 25% more time is used collecting data with empty targets at each setting. A 2% interaction length carbon target is about 1 cm thick. The MINOS, atmospheric neutrino, and hadroproduction generator programs have a large number of data points in common. The total number of triggers which will be collected is around 10^7 which will take a total of 12 weeks running to collect including the empty target runs.

6.2 Financial expenditure

No significant modifications of the existing NA49 apparatus are envisaged, except the construction of suitable targets and adaptation of target holders. This work will be performed by workshops of participating institutes. The estimated total expenditure (see Table 2) is 50 kCHF. Our programme foresees the use of carbon targets for the main measurements. We retain the option of using cryogenic N_2 targets using the HARP cryogenic target equipment. This choice will be made based on the experience with cryogenic targets in HARP running in 2001, and 20 kCHF is included in the investment

	Cost (kCHF)
Target and target holder materiel	10
Miscellaneous	20
HARP cryogenic target modification (optional)	20
Total	50

Table 2: Investment expenditure

expenditure in case we need to adapt these targets for use in NA49.

The exploitation expenses are shown in Table 3. They are based on well known NA49 operating costs and are estimated for 6 weeks of running in each of 2002 and 2003. Annual electronics rental fees and maintenance costs are divided equally between this proposed activity and the NA49 programme of operation in heavy ion beams. NA49 proper is approved for running in 2001 and 2002 and envisages to also participate in the heavy ion run in 2003 (see CERN/SPSC 2001-008). Column (A) in Table 3 assumes that the NA49 heavy ion programme extends into 2003. Column (B) lists the figures if this collaboration must fund 100% of the electronics pool and maintenance costs after the NA49 lead-ion run in 2002.

	Cost (kCHF)	
	(A)	(B)
Gases	70	70
Electronics rental fee (EP Pool)	60	90
Data recording media	80	80
Maintenance, repairs	50	75
Subsistence of experts (20 months)	80	80
Total	340	395

Table 3: Exploitation expenditure. Column (A) assumes that the NA49 lead ion programme extends into 2003. Column (B) assumes this collaboration must fund 100% of the electronics pool and maintenance costs after the NA49 lead-ion run in 2002.

This estimate assumes that the agreements of the NA49 collaboration with CERN as host laboratory remain in force until the end of 2003. It has been agreed that the investment and exploitation costs will be equally shared between those institutes which are primarily interested in the atmospheric neutrino flux, and those institutes which are primarily interested in the hadron-production properties of the NuMI target. The collaborators from the NA49 experiment who will participate in this measurement are considered to have made the in-kind contribution of the NA49 detector itself and will not contribute to the specific investment and exploitation funds required for this proposal.

6.3 Manpower needs

The running of the experiment depends to a very large extent on the availability of key experts from the NA49 collaboration. These have been identified and are authors of this proposal. They provide essential expertise for operating and maintaining the hardware, supervise the data taking, assure online quality control, and take responsibility for data reduction up to and including event reconstruction.

The key experts are to a large extent members of Eastern European institutes, whose presence at CERN would have to be assured by the collaboration by way of monthly subsistence payments. The corresponding expenditure is included in Table 3.

7 Conclusion

To summarise, the NA49 experiment can be used to significantly improve the coverage of the phase space of the world's hadroproduction data. This data is vital to improve the understanding of the rate and spectra of neutrinos, both those produced in the atmosphere and those projected towards the MINOS detectors from the NuMI beam at Fermilab. The data will also provide substantial new input to hadroproduction Monte Carlo generators which are used in both the design and analysis phases of all modern high energy physics experiments. The data can be collected with minimal modification to the existing NA49 apparatus with 12 weeks of total running time which is most conveniently taken in two periods, one in 2002 and one in 2003.

References

[1] S. Afanasiev *et al.*, (NA49 Collaboration), "The NA49 large acceptance hadron detector," Nucl. Instrum. Meth. **A 430** (1999) 210.

[2] MINOS Technical Design Report, NuMI-L-337 (1998). (Available from `http://www.hep.anl.gov/ndk/hypertext/numi_notes.html`)

[3] NuMI Facility Technical Design Report, NuMI-L-346 (1998).

[4] H. Atherton *et al.*, **CERN 80-07**, (1980).

[5] D. Barton *et al.*, Phys. Rev. **27** (1983) 2580.

[6] G. Ambrosini *et al.*(SPY Collaboration), Phys. Lett. **B420** (1998) 225; Phys. Lett. **B425** (1998) 208; Eur. Phys. J. **C10** (1999) 605.

[7] R. Brun, F. Bruyant, A.C. McPherson, P. Zanarini, CERN Data Handling Division, DD/EE/84–1, 1987; CERN Program Library, W5013 (1994).

[8] M. Bonesini, A. Marchionni, F. Pietropaolo and T. Tabarelli de Fatis, Eur. J. Phys. C, DOI 10.1007/S100520100656 (hep-ph/0101163).

[9] N.V. Mokhov and S.I. Striganov, "Model for Pion Production In Proton-Nucleus Interaction", AIP Conf. Proc. **435** (1997) 543. N.V. Mokhov, The MARS Code System User's Guide, Version 13(95), Report Fermilab-FN-628 (1995); http://www-ap.fnal.gov/MARS/

[10] A.J. Malensek, Fermilab-FN 341, (1981).

[11] HARP collaboration, "Proposal to study hadron production for the neutrino factory and for the atmospheric neutrino flux", CERN/SPSC/99-35/P315 (15 November 1999), [Expt. PS214 HARP].

[12] Super–Kamiokande collaboration, Y. Fukada *et al.*, Phys. Rev. Lett. **81** (1998) 1562.

[13] V. Agrawal, T.K. Gaisser, P. Lipari, T. Stanev, Phys. Rev. **D53** (1996) 1314.

[14] M. Honda, T. Kajita, K. Kasahara, S. Midorikawa, Phys. Rev. **D52** (1995) 4985.

[15] G. Battistoni, A. Ferrari, P. Lipari, T. Montaruli, P.R. Sala, T. Rancati, 'A 3-Dimensional Calculation of Atmospheric Neutrino Flux', Astroparticle Physics **12** (2000) 315, hep-ph/9907408

[16] P. Lipari, 'The primary protons and the atmospheric neutrino fluxes', hep-ph/9905506.

[17] G. Battistoni, 'Uncertainties on Atmospheric Neutrino Flux Calculations', Nucl. Phys. Proc. Suppl. **100** (2001) 101, hep-ph/0012268.

[18] A recent compilation of cosmic ray fluxes is given in T. K. Gaisser, astro-ph/0104327.

[19] HARP collaboration, "Proposal to study helium-induced hadron production for the atmospheric-neutrino flux", CERN/SPSC/2001-016, SPSC/P315 Add.1.

[20] R. Engel, T. K. Gaisser and T. Stanev, Phys. Lett. **B472** (2000) 113.

[21] P. Aarnio *et al.*, Report CERN/TIS-RP/93-10; A. Ferrari and P.R. Sala, Proc. Workshop on Nuclear Reaction Data and Nuclear Reactors Physics, Design and Safety, ICTP (Trieste, Italy), April 1996, World Scientific (eds. A. Gandini and G. Reffo), p. 424; A. Fassò *et al.*, Proc. 3rd Workshop on Simulating Accelerator Radiation Environments, KEK (Tsukuba, Japan), May 1997, KEK Proceedings 97-5 (ed. H. Hirayama), p. 32; and references cited therein.

[22] The GEANT 4 Collaboration, CERN/DRDC/94–29, DRDC/P58 1994.

[23] H.C. Fesefeldt, Simulation of hadronic showers, physics and application, Technical Report PITHA 85–02, 1985.

[24] C. Zeitnitz and T.A. Gabriel, GEANT-CALOR Interface Users̀ Guide, ORNL, 1996.

[25] A. Ferrari and P.R. Sala, ATLAS Internal Note PHYS-No-086 (June 1996).

[26] G. Collazuol *et al.*, Report CERN-OPEN-98-032; Nucl. Instr. and Meth. **A449** (2000) 609.